Nazgul A. Yessentayeva* [ID], Aldana R. Galiyeva [ID], Arailym T. Daribay [ID], Daniyar T. Sadyrbekov [ID], Tolkyn S. Zhumagalieva [ID], Dias T. Marsel [ID]

Karaganda Buketov University, Karaganda, Kazakhstan
(*Corresponding author's e-mail: naz.yessentayeva92@gmail.com)

Synthesis and Optimization of Bovine Serum Albumin Nanoparticles Immobilized with Antituberculosis Drugs

This study involved the synthesis of bovine serum albumin (BSA) nanoparticles immobilized with the antituberculosis drugs isoniazid (INH) and rifampicin (RIF) by the desolvation method. The primary objective was to explore the impact of varying concentrations of albumin, urea, cysteine, rifampicin, and isoniazid on the average size of nanoparticles, polydispersity, and the encapsulation efficiency of drugs. The study's outcomes affirm that alterations in the concentrations of these components influence nanoparticles' parameters, highlighting their key role in optimizing the encapsulation process and enhancing the efficacy of tuberculosis drug delivery. The nanoparticles obtaned as a result of optimization demonstrated an optimal size of 231.2±1.2 nm with a polydispersity of 0.061±0.08. Encapsulation efficiency was 89% for rifampicin and 38.5% for isoniazid. The investigation of drug release kinetics from the polymer matrix revealed a gradual release pattern. Evaluation of the obtained nanoparticles by Fourier-transform infrared spectroscopy (FTIR), thermogravimetric analysis (TGA), and differential scanning calorimetry (DSC) confirmed the successful incorporation of drugs into the polymer matrix. These findings highlight the potential of BSA nanoparticles as effective carriers for tuberculosis treatment, with implications for refining drug delivery strategies.

Keywords: nanoparticles, bovine serum albumin, rifampicin, isoniazid, desolvation, hydrophilic drugs, hydrophobic drugs, anti-tuberculosis drugs.

Introduction

Addressing tuberculosis remains a considerable medical hindrance, considering its persistent threat to human health, especially in regions with a high incidence of the disease. Millions of people are diagnosed with tuberculosis annually, and the development of effective treatment methods remains a pressing task [1]. However, successful tuberculosis treatment requires precise dosing and prolonged use of medications, often accompanied by side effects and low treatment adherence. In this regard, innovative strategies for delivering antituberculosis drugs have become a priority. Furthermore, the increasing resistance of microorganisms to existing antituberculosis medications emphasizes the urgent need to explore new approaches to combat the infection [2–4].

Overcoming resistance to antituberculosis drugs is a critically important task in the fight against tuberculosis, especially when there is multidrug-resistant (MDR) and extensively drug-resistant (XDR) strains. One of the methods that can help to overcome resistance to antituberculosis drugs is the use of drug combinations, as well as the use of nanoparticles as carriers for antituberculosis drugs. This approach has the potential to enhance their effectiveness and facilitate penetration into Mycobacterium tuberculosis [5, 6].

Taking this into account, bovine serum albumin (BSA) can be identified as a promising material for the synthesis of nanoparticles serving as drug carriers. Bovine serum albumin, a protein extracted from bovine serum, possesses a significant potential for creating nanoparticles that can act as carriers for antituberculosis drugs [7]. The immobilization of antituberculosis drugs such as rifampicin and isoniazid into nanoparticles based on bovine serum albumin represents a prospective approach to enhance the delivery and effectiveness of medications in tuberculosis treatment. Rifampicin and isoniazid (Fig. 1) are widely used in combination for tuberculosis treatment. Their combination can increase efficacy and reduce the probability of drug resistance development among disease-causing agents. Immobilizing both drugs into nanoparticles based on albumin can provide a synergistic effect and optimize treatment [8, 9].

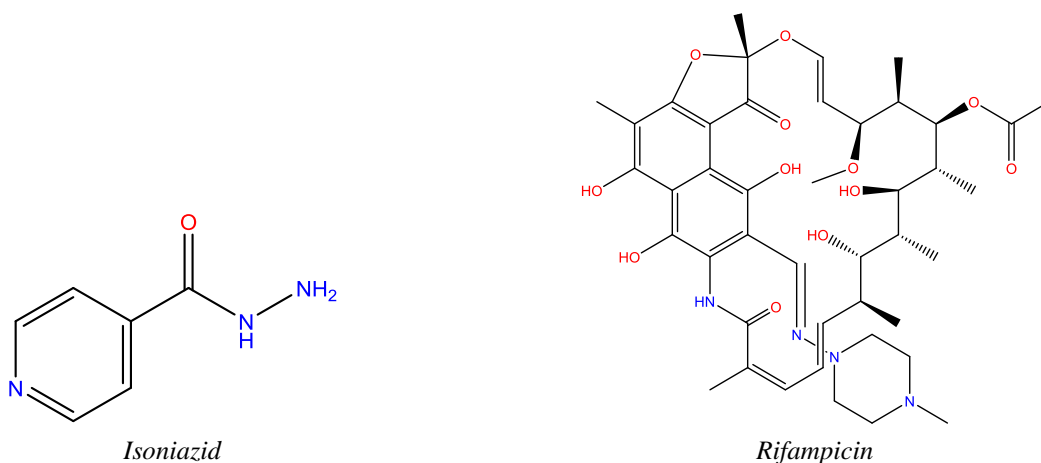*Isoniazid*   *Rifampicin*

Figure 1. Chemical Structure of antituberculosis drugs

The aim of this study is the creation and optimization of nanoparticles based on bovine serum albumin (BSA), immobilized with rifampicin (RIF) and isoniazid (INH). Thus, in this work, we investigated for the first time the influence of technological parameters on the characteristics of particles (average size, polydispersity) of BSA nanoparticles loaded with rifampicin and isoniazid (BSA-RIF-INH NPs), as well as on the production efficiency (binding efficiency and yield). Furthermore, the physicochemical characteristics of the obtained nanoparticles and the in vitro drug release profile from the polymer matrix were examined.

Experimental

Materials

Bovine serum albumin (lyophilized powder, 98 %) (BSA) was purchased from Sigma Aldrich, Urea (99.5 %) was obtained from ChemPriborSPb (St. Petersburg, Russia), L-cysteine (98.5 %) and Isoniazid (99 %) (INH) was acquired from Sigma Aldrich, Ethanol was received from DosFarm (Almaty, Kazakhstan), Rifampicin (Sigma Aldrich), Potassium dihydrophosphate and sodium hydrophosphate were used to prepare a phosphate-buffered saline solution.

Preparation of INH and RIF loaded BSA NPs

BSA nanoparticles loaded with INH and RIF were prepared using a modified desolvation method, as described previously [6, 10]. In summary, aqueous solution of BSA with required concentration was prepared by dissolving BSA powder in 3 mL of distilled water (pH 7.4) on magnetic stirrer at 200 rpm. After that, 0.5 mL of a urea solution was introduced into the BSA solution, and the mixture was then sonicated for 3 minutes. Because RIF exhibits minimal solubility in water, it was incorporated by dissolving it in a mixture of DMSO and water (volume concentration of DMSO was 20 %) along with INH. Subsequently, the resulting mixture was introduced into the original BSA-Urea solution. Then, ethanol was gradually incorporated into the solution at a rate of 1 mL/min, with continuous stirring (at 200 rpm, at room temperature), until achieving a turbid dispersion. This turbidity signified the formation of BSA nanoparticles containing INH and RIF. Finally, 3 mL of a L-cysteine solution was added. The stirring process persisted for a duration of two hours, after which the resultant nanoparticles were isolated through centrifugation (MiniSpin, Eppendorf, Hamburg, Germany) at 14 000 rpm for 30 minutes. This was followed by a two-step washing procedure using distilled water to clean the nanoparticles from residual ethanol and drugs not encapsulated within the BSA.

Particle size, polydispersity index of the BSA-RIF-INH NPs'

The size of the nanoparticles (diameter) and their distribution (polydispersity index) were assessed using dynamic light scattering (DLS) with a laser-based particle size detector (Malvern Zetasizer Nano S90, Malvern Instruments Ltd., Malvern, UK). Obtained colloidal suspension was diluted with distilled water and the average size and PDI measurement was carried out. The measurements were provided three times at 25 °C, and results were presented as an average value ± standard deviation.

Encapsulation efficiency and BSA-RIF-INH NPs' yield

After centrifugation and rinsing the nanoparticles the supernatant was collected and analyzed using high-performance liquid chromatography (HPLC) with a Shimadzu LC-20 Prominence instrument, with the aim of quantifing the mass of rifampicin and isoniazid that remained unencapsulated in BSA nanoparticles. The encapsulation efficiency and nanoparticles' yield were then determined using the formulas given below:

$$\text{Encapsulation efficiency}\,(\%) = \frac{\text{Total mass of drug} - \text{mass of free drug}}{\text{Total mass of drug}} \times 100\,\%$$

$$\text{Nanoparticles Yield}\,(\%) = \frac{\text{Total mass of NPs}}{\text{Total mass of INH} + \text{Total mass of RIF} + \text{Total mass of BSA}} \times 100\,\%$$

In vitro release of RIF and INH from polymer NPs

The release characteristic of rifampicin and isoniazid from BSA nanoparticles was studied in phosphate-buffered saline (PBS, pH 7.4). Briefly, 24 mg of RIF-INH-BSA NPs were dissolved in 14 mL PBS with pH 7.4 and were incubated at 37 °C under constant stirring (200 rpm). At certain intervals, which were equal to 15 min, 30 min, 1, 2, 4, 8 and 24 h, 1 mL of sample was collected and centrifuged, following HPLC analysis to identify the concentration of released drug. The amount of released RIF and INH was calculated using the following formula:

$$\text{Drug release}\,(\%) = \frac{\text{Mass of drug}\,(\text{INH or RIF})\,\text{released}}{\text{Mass of the total drug}\,(\text{INH or RIF})\,\text{in nanoparticles}} \times 100\,\%$$

Thermogravimetric analysis and differential scanning calorimetry

The thermal decomposition properties of BSA-RIF-INH nanoparticles were examined through thermogravimetric analysis and differential scanning calorimetry (LabSYS evo TGA/DTA/DSC, Setaram, France). The investigation was conducted employing a simultaneous approach involving thermogravimetry and differential scanning calorimetry. A quantity of 10 milligrams of the sample was employed for the analysis. The study was carried out in an open crucible, since the primary methodology was focused on thermal stability. In the differential scanning calorimetry area, the second crucible was intentionally left empty. The estimation was made under a nitrogen atmosphere with a flow rate of 30 mL/min, and the temperature was increased at a rate of 10 °C/min, covering a range from 30 °C to 600 °C.

Study of prepared nanoparticles by infrared spectroscopy

Infrared spectroscopy (FSM 1202, Infraspek Ltd., Russia) was used to identify the samples. The FTIR spectra were obtained by the KBr method, which involves creating a pellet by mixing 3 mg of the sample with 100 mg of KBr. The analyzed IR range extended from 4000 to 400 cm^{-1}.

Statistical Analysis

Experiments were carried out in triplicate, and the findings are presented as the mean values along with their respective standard deviations (SD). Statistical evaluations were carried out employing the Student's t-test through Statistica 12 (TIBCO Software Inc., Palo Alto, CA, USA). A significance threshold of 0.05 was employed to ascertain statistical significance.

Results and discussion

In previous studies, the possibility of obtaining stable BSA nanoparticles by the synergistic interaction of urea and L-cysteine with the protein, including the immobilization of isoniazid, has been demonstrated [6]. Within the scope of this research, the potential for obtaining BSA nanoparticles using biocompatible components and immobilizing antituberculosis drugs — isoniazid and rifampicin — will be explored. BSA nanoparticles were obtained sequentially using the desolvation method with urea and cysteine, and the immobilization of drugs was carried out using the encapsulation method. Schematic representation of preparation method of BSA-RIF-INH nanoparticles is presented in Figure 2.
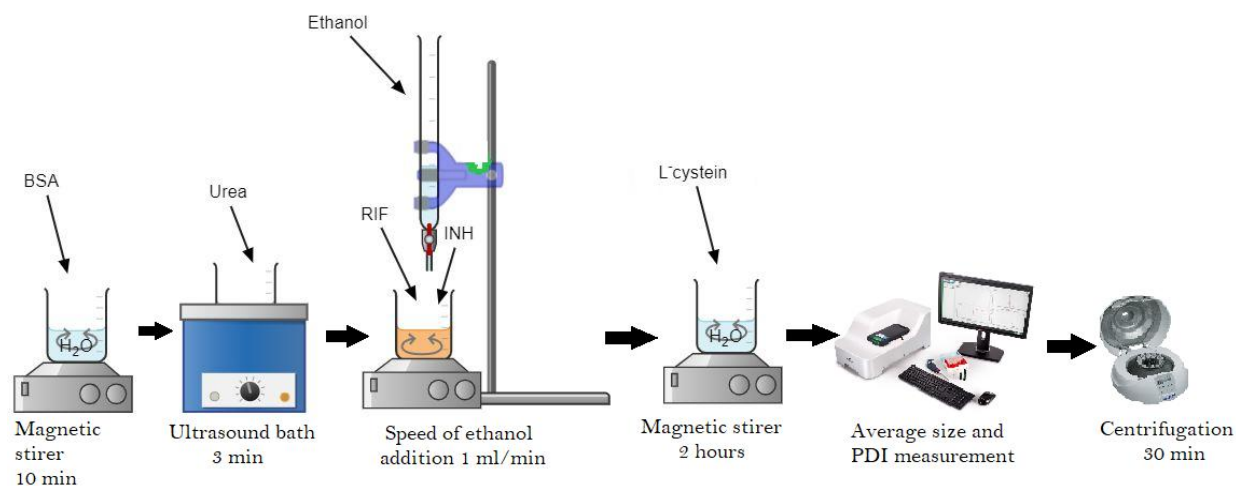
Figure 2. Schematic representation of preparation method of BSA-RIF-INH nanoparticles

Study the effect of urea and L-cysteine on NP characteristics

Urea is a chaotropic agent, aiding in the disruption of hydrophobic interactions within the protein, thereby enhancing its solubility [11]. The urea concentration affects such characteristics of nanoparticles as size, shape and dispersity. To investigate the effect of urea on nanoparticles' characteristics, the nanoparticles were synthesized under the following conditions (standard conditions): BSA concentration 60 mg/mL; L-cysteine concentration 1 mg/mL; pH 7.4; RIF and INH concentrations of 10 mg/mL each, respectively, with ethanol as the desolvating agent. The prepared nanoparticles were characterized using photon correlation spectroscopy (Fig. 3).
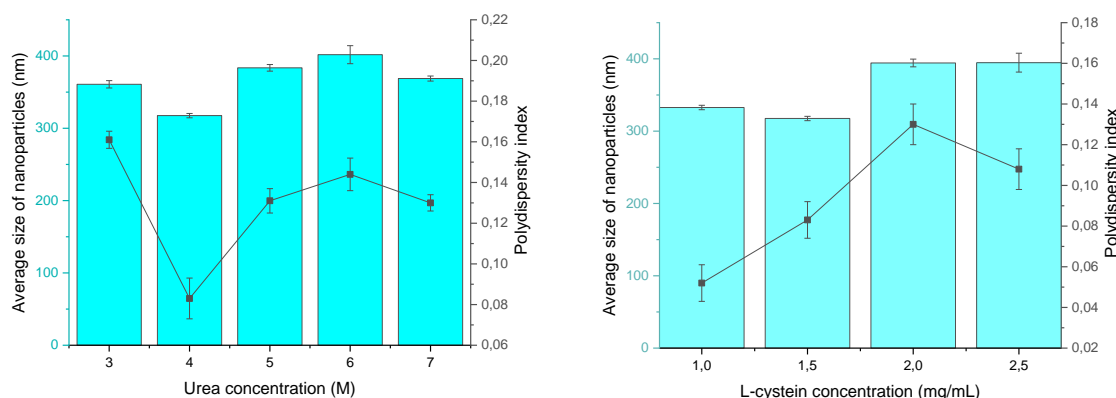

Figure 3. Influence of urea and L-cysteine on the average size and polydispersity of nanoparticles

The graph reveals a trend where the average nanoparticle size initially increases as the urea concentration rises from 4 M to 6 M. This phenomenon is likely associated with particle aggregation at higher urea concentrations. The smallest average nanoparticle size (317.5±3) and the lowest polydispersity (0.083±0.010) are achieved at a urea concentration of 4 M.

The use of L-cysteine in albumin nanoparticles for thiol-disulfide exchange represents an innovative method that can find applications in various fields, including medicine and biotechnology [7]. Cysteine contains a thiol functional group (-SH) capable of forming disulfide bonds (-S-S-) with other thiol molecules. This process can be used to control the delivery and release of drugs. The thiol groups of cysteine react with the disulfide bridges which present in the structure of albumin, ensuring a robust immobilization of drugs [7, 12]. Figure 3 illustrates the results of the impact of L-cysteine on the characteristics of BSA-RIF-INH nanoparticles.

With an increase in cysteine concentration from 1.5 to 2.5 mg/mL, the average size of nanoparticles increases from 317.47±3 nm to 394.7±13 nm. Additionally, the polydispersity index increases with the rise of the concentration of cysteine. The observed phenomenon might be attributed with the excess of L-cysteine,

which induces a reduction in the intermolecular S-S bridges that are formed. This, in turn, disrupts the evolving three-dimensional gel-like structure of albumin. As a consequence, larger particles may unfold, leading to an increase in both the formation of macrostructures and the values of the dispersion index [7].

Study the effect of albumin concentration on NP characteristics

Different concentrations of BSA (10, 20, 40, 60, and 80 mg/mL) were used during the nanoparticles' synthesis to investigate its influence on the characteristics of BSA nanoparticles and determine the optimal concentration of BSA. Table 1 illustrates the effect of polymer concentration on the size and encapsulation efficiency of nanoparticles loaded with RIF and INH at a urea concentration of 4 M and cysteine concentration of 1 mg/mL.

T a b l e 1

Effect of the BSA concentration on nanoparticle size, PDI, encapsulation efficiency and yield

BSA concentration (mg/mL)	Average size of nanoparticles (d, nm)	PDI	Encapsulation efficiency (%)		Yield (%)
			Rifampicin	Isoniazid	
20	164.5±0.9	0.098±0.021	67±4	43±3	17±3
40	194.2±2.1	0.122±0.019	67±2	37±2	15±4
60	214.8±1.7	0.139±0.016	70±4	50±3	36±4
80	339.5±1.1	0.159±0.013	69±2	44±3	31±2

The nanoparticle size increases from 164.5±0.9 to 339.5±1.1 nm, and the drug content percentage rises from 67±4 to 70±4 % for rifampicin and from 37±2 to 50±3 % for isoniazid as the albumin concentration increases from 10 to 80 mg/mL. The obtained results indicate that the polymer concentration predominantly influences the size and drug binding efficiency of the loaded nanoparticles. Polymer concentration is a key factor affecting the nanoparticle characteristics. Higher polymer concentration increases the average size and encapsulation efficiency, consistent with the findings of many other studies [13]. An increase in polymer concentration causes a rise in the viscosity of the dispersed phase, leading to the formation of larger droplets and a deceleration in the diffusion rate of BSA into the surrounding aqueous phase. Thus, the viscosity of the polymer solution significantly influences the nanoparticle size. A polymer concentration of 60 mg/mL provided the highest yield of nanoparticles — 36±4%.

Study the effect of anti-tuberculosis drugs concentration on the formation of nanoparticles (NPs)

Investigating the effect of drug concentration in the polymer matrix on the average size is a crucial aspect of drug carrier development. Rifampicin and isoniazid, serving as representative bioactive compounds, were immobilized into BSA nanoparticles. The immobilization process involved their incorporation in the synthesis of BSA nanoparticles, which were effectively formed using natural cross-linking agents like albumin, urea, and L-cysteine. The concentration of the drugs ranged from 2 to 10 mg/mL, and the outcomes are outlined in Table 2.

T a b l e 2

Effect of the concentration of rifampicin on nanoparticles' size, PDI, encapsulation efficiency and yield

Rifampicin concentration (mg/mL)	Average size of nanoparticles (d, nm)	PDI	Encapsulation efficiency of Rifampicin (%)	Yield (%)
2	106.3±1.1	0.380±0.008	86±3	3±2
4	161.7±0.9	0.173±0.014	88±5	13±4
6	254.3±1.5	0.110±0.044	92±5	41±5
8	381.6±1.4	0.240±0.009	91±2	55±2
10	317.5±3.1	0.083±0.010	81±2	51±3

The results presented in Table 2 indicate a significant influence of the drug concentration on the key characteristics of the system. The research results reveal that changes in rifampicin concentration lead to variations in the average particle size. Thus, with an increase in rifampicin concentration, the average particle size increases from 106.3±1.1 to 381.6±1.4 nm. The highest degree of binding was observed at a drug content of 6 mg/mL, reaching 92±5 %.

Table 3 presents the particle sizes and the degree of binding of nanoparticles loaded with anti-tuberculosis drugs prepared with different concentrations of isoniazid (2, 4, 6, 8, and 10 mg/mL).

As reflected in Table 3, increasing the concentration of isoniazid significantly affected the particle size and the encapsulation efficiency of the drug. As the concentration of isoniazid increases the average particle size decreased from 179.9±1.1 % to 161.7±0.9 nm. This trend confirms that the concentration of isoniazid directly influences the particle size, leading to their reduction in agreement with the results observed by Tazhbayev Y. and Galiyeva A. [10]. Moreover, the encapsulation efficiency of isoniazid increased with its concentration, reaching 40±5 % at a concentration of 10 mg/mL. These results highlight the importance of optimizing the isoniazid concentration to achieve the desired physicochemical characteristics of nanoparticles and ensure effective binding to the carrier.

T a b l e   3

Effect of the isoniazid concentration on nanoparticles' size, PDI, encapsulation efficiency and yield

Isoniazid concentration (mg/mL)	Average size of nanoparticles (d. nm)	PDI	Encapsulation efficiency of Isoniazid (%)	Yield (%)
2	179.9±1.1	0.125±0.010	32±4	14±4
4	175.3±1.4	0.139±0.007	30±2	12±5
6	172.2±1.6	0.197±0.008	39±2	8±1
8	164.5±0.8	0.152±0.016	39±3	12±4
10	161.7±0.9	0.173±0.014	40±5	13±3

The recommended strategy involves the production of particles with a size below 300 nm, as this offers favorable pharmacological traits, prolonged circulation kinetics, and a gradual release specifically in targeted regions. Throughout this investigation, a thorough exploration of the impact of reagent concentrations on BSA-RIF-INH NPs properties was conducted. Following optimization, the ideal parameters were identified: BSA — 60 mg/mL, urea — 4 M, L-cysteine — 1.5 mg/mL, isoniazid — 10 mg/mL, rifampicin — 6 mg/mL. BSA-RIF-INH NPs exhibited an average size of 231.2±1.2 nm with a polydispersity of 0.061±0.08 (Fig. 4). Successful completion of the encapsulation process was confirmed by obtaining noteworthy encapsulation efficiency (89 % for rifampicin and 38.5 % for isoniazid).
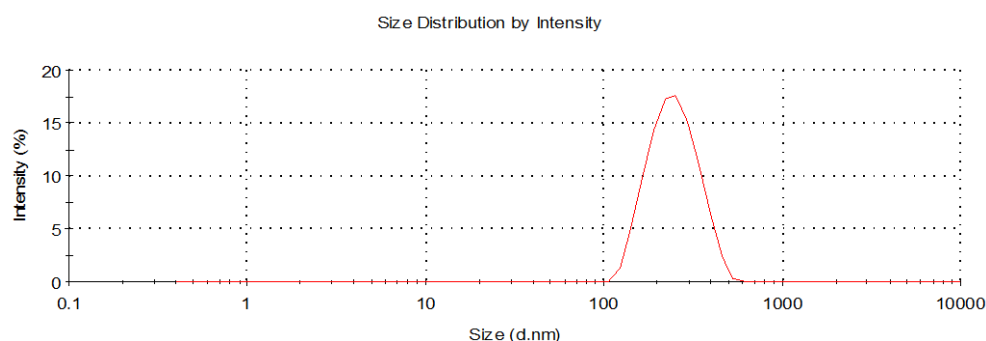

Figure 4. Particle size of optimized BSA-RIF-INH nanoparticles determined by photon correlation spectroscopy

To validate the encapsulation of the rifampicin and isoniazid into the BSA NPs, thermogravimetric analysis (TGA) and differential scanning calorimetry (DSC) were conducted. Thermograms of these drugs, BSA NPs and BSA-RIF-INH NPs are illustrated in Figure 5.

According to the graph, rifampicin, as polymorph I, remains thermally stable up to 230 °C. Its thermal decomposition process takes place in two stages [10, 15]. At the first stage, which occurs between 230–285 °C, there is a sharp mass loss of 22 %. Then during the second stage, in the interval 285–617 °C, the mass of RIF decreases more smoothly for 28 %. The distinct endothermic peak for isoniazid is detected at 175.6 °C, which corresponds to the melting point, since the mass of INH remains unchanged. The decomposition of this drug occurs between 257 °C and 445 °C, with a 75 % reduction in INH mass [10, 14]. Three endothermic peaks at 94.4, 245.8 and 390.7 °C are noted on the DSC curve for BSA NP. Considering that the albumin molecule has three different domains [6, 16], its thermal denaturation on the TGA curve presents three characteristic transitions, the mass loss at the end of all stages of decomposition equals to 82 %. Endo-

thermic peaks for BSA-RIF-INH NPs are detected at 92.9, 224 and 361.5 °C, which corresponds to the decrease of NPs' mass in the TGA curve; the mass loss is 44 %. Nevertheless, a noticeable displacement of peaks to lower temperature range is noticed in contrast to the curves of empty BSA NPs. This could be attributed to the influence of medications.
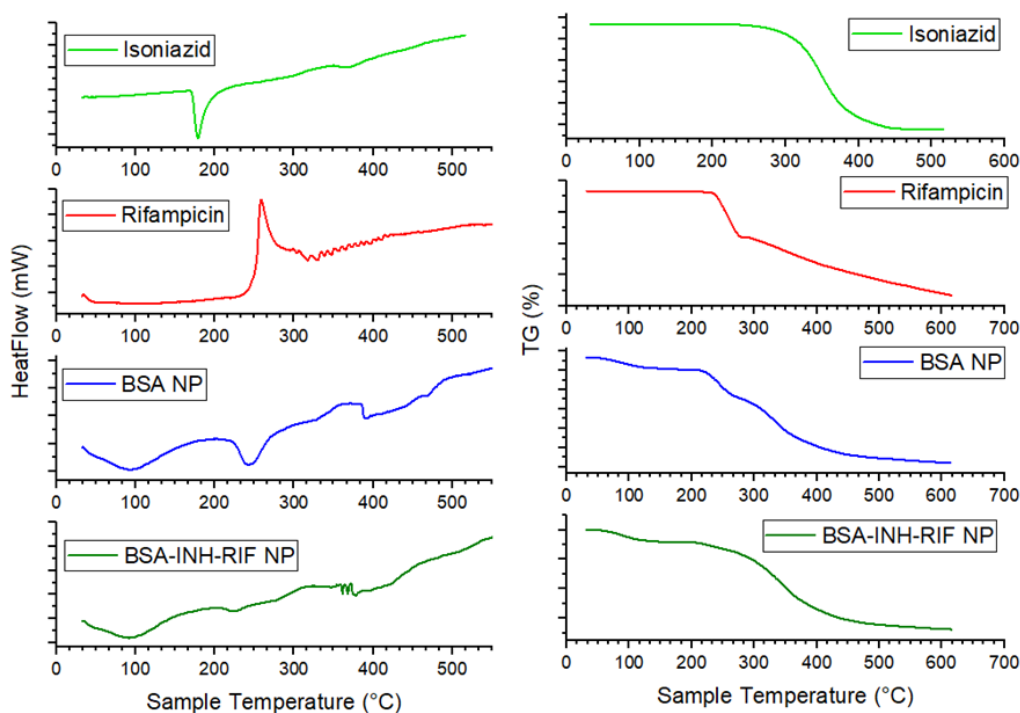

Figure 5. Differential scanning calorimetry and thermogravimetric analysis
of Rifampicin, Isoniazid, BSA NPs, BSA-INH-RIF NPs

FT-IR spectra were obtained for BSA nanoparticles, BSA-RIF-INH nanoparticles, rifampicin and isoniazid, as depicted in Figure 6. These spectra reveal distinct bands corresponding to specific wavenumbers, identifying characteristic features of the original albumin. Significantly, key peaks include 3418 cm^{-1} is indicative of the A-amide group linked to N–H, while the following prominent peak at 2824 cm^{-1} identifies the B-amide group associated with free ion. The peak at 1489 cm^{-1} represents Amide II, indicating C–N stretching and N–H bending vibrations. Amide I, linked to the C–O bond, is denoted by the peak at 1620 cm^{-1}, and the presence of CH$_2$ groups is evident at 1392 cm^{-1}. Additionally, the observation of amide III at around 1335 cm^{-1} is associated with –C–N– group stretching and N–H bending vibrations [6; 7].
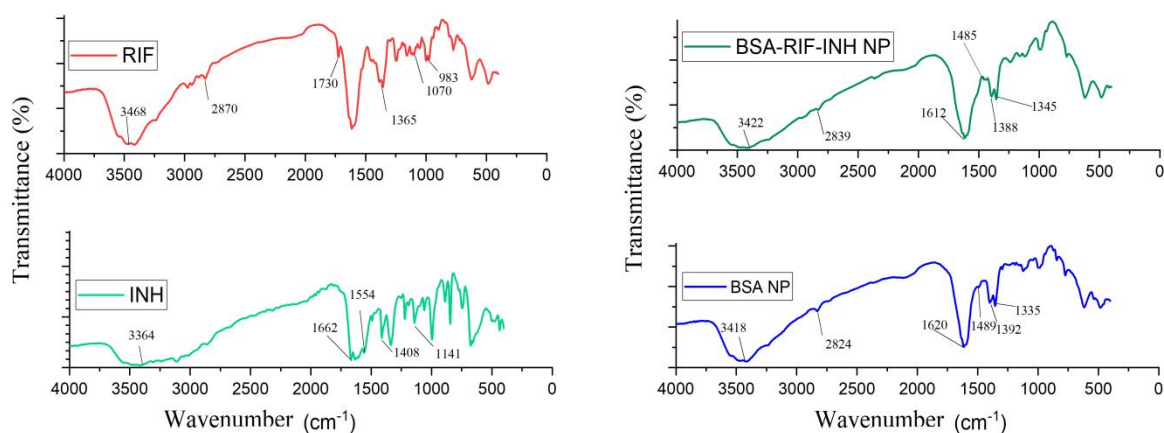

Figure 6. FT-IR spectra of the isoniazid, rifampicin, BSA NPs and BSA nanoparticles
immobilized with rifampicin and isoniazid

In case of rifampicin, significant absorption features are observable: a distinct peak at 983 cm^{-1} denotes $\equiv$C-H, C-H bond, 1070 cm^{-1} is linked to –CH, CO, and C-H, the peak at 1365 cm^{-1} is associated with the CH_2 and C=C. The peak at 3468 cm^{-1} connected to NH stretching, 2870 cm^{-1} is linked to the C–H bond, and 1730 cm^{-1} is related to the C=O bond [10, 18, 19]. The FTIR spectrum of isoniazid exhibits clear peaks at different wavenumbers: 3364 cm^{-1} signifies the N-H bond, 1662 cm^{-1} (C=O) is associated with pyridine, 1554 cm^{-1} is related to the –C–N bond, and the peak at 1141 cm^{-1} corresponds to the –N–N amide group [6, 10, 17]. The FTIR spectrum associated with BSA-RIF-INH NPs closely resembled that of the BSA NPs. The absence of distinct peak characteristics for rifampicin and isoniazid in the FTIR spectra of final NPs, concealed by polymer bands, suggests successful embedding of the drugs within the nanoparticles [6, 18].

To validate the sustained effect of the synthesized nanoparticles, it is essential to explore the kinetics of drug release from complexes formed by loading rifampicin and isoniazid into polymers. The release of RIF and INH from produced nanoparticles was studied in phosphate buffer saline (PBS) with a pH of 7.4. The evaluation of RIF and INH release from the nanoparticles was quantified by measuring the concentration of the released drug, as determined using HPLC. The results of this analysis are visually depicted in Figure 7, providing a clear representation of the extent of drug release over time.
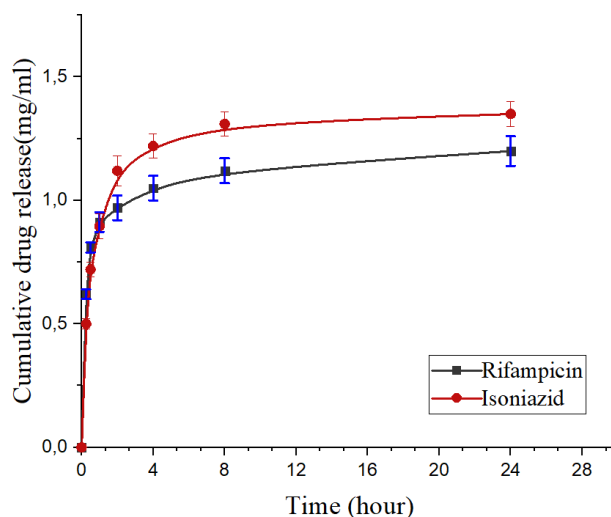

Figure 7. Investigation of INH and RIF release from the polymer matrix in phosphate-buffered saline

The graph illustrated in Figure 7 demonstrates a constant and persistent release of medicines from obtained nanoparticles throughout the entire investigation period of 24 hours. At the end of experiment period the concentrations of RIF and INH equaled to 1,2 and 1,35 mg/mL respectively. This highlights the considerable potential for the prolonged release of isoniazid and rifampicin from albumin nanoparticles. The investigation of release kinetics reveals a minor initial burst effect followed by an extended and gradual release of rifampicin and isoniazid. It could be attributed to the medicine adsorbed on the surface of the BSA-INH-RIF nanoparticles [6, 7], followed by a diffusion process through the polymer matrix of the nanoparticles, consistent with the findings reported by Mandhar, P. and Joshi, G. [20]. Such sustained release capabilities offer the advantage of preventing abrupt spikes in drug concentration in the bloodstream, ensuring therapeutic levels are maintained over an extended period. This highlights the potential of these particles as effective carriers for delivering isoniazid and rifampicin [14, 21, 22].

Conclusion

The effects of urea, L-cysteine, bovine serum albumin, isoniazid and rifampicin concentrations were carefully analyzed in this study. It was found that polymer and rifampicin concentrations had a significant effect on the key characteristics of the nanoparticles. The optimization process produced nanoparticles with desired parameters such as size (231.2±1.2 nm) and polydispersity (0.061±0.08). The degree of drug binding was 89 % for rifampicin and 38.5 % for isoniazid. The results suggest the possibility of sustained drug release both in vitro and in vivo, emphasizing the potential of bovine serum albumin nanoparticles as a promis-

ing carrier for anti-TB drugs. These findings provide important indications for future research and practical applications of this technology in the field of drug delivery.

Author Information*

_____

*The authors' names are presented in the following order: First Name, Middle Name and Last Name

Nazgul Asylbekkyzy Yessentayeva (*corresponding author*) — 2nd year Doctoral Student, Department of Organic Chemistry and Polymers, Karaganda Buketov University, Universitetskaya street, 28, 100024, Karaganda, Kazakhstan.; e-mail: naz.yessentayeva92@gmail.com; https://orcid.org/0000-0003-4820-8460

Aldana Rymzhanovna Galiyeva — Engineer, Institute of Chemical Problems, Karaganda Buketov University, Universitetskaya street, 28, 100024, Karaganda, Kazakhstan; e-mail: aldana_karaganda@mail.ru; https://orcid.org/0000-0002-8551-6297

Arailym Turashkyzy Daribay — Master Student, Karaganda Buketov University, Universitetskaya street, 28, 100024, Karaganda, Kazakhstan; e-mail: arailymdaribay@gmail.com; https://orcid.org/0000-0001-5675-0351

Daniyar Tleuzhanovich Sadyrbekov — Candidate of Chemical Sciences, Researcher, laboratory of the engineering profile "Physical and chemical methods of research", Karaganda Buketov University, Universitetskaya street, 28, 100024, Karaganda, Kazakhstan; e-mail: acidbear@mail.ru; https://orcid.org/0000-0002-3047-9142

Tolkyn Sergaziyevna Zhumagalieva — Professor of the Department of Organic Chemistry and Polymers, Karaganda Buketov University, Universitetskaya street, 28, 100024, Karaganda, Kazakhstan; e-mail: zhumagalieva79@mail.ru; https://orcid.org/0000-0003-1765-752X

Dias Temirlanuly Marsel — Master Student, Karaganda Buketov University, Universitetskaya street, 28, 100024, Karaganda, Kazakhstan; e-mail: marsel.dias@bk.ru; https://orcid.org/0000-0002-1204-0814

Author Contributions

The manuscript was written through contributions of all authors. All authors have given approval to the final version of the manuscript. CRediT: **Aldana Rymzhanovna Galiyeva** conceptualization, data curation, methodology; writing — review and editing; **Nazgul Asylbekkyzy Yessentayeva** writing — original draft, writing-review and editing, investigation, data curation: **Tolkyn Sergaziyevna Zhumagaliyeva** data curation, writing — review and editing; **Arailym Turashkyzy Daribay** investigation, resources**; Daniyar Tleuzhanovich Sadyrbekov** investigation; **Dias Temirlanuly Marsel** investigation.

Conflicts of Interest

The authors declare no conflict of interest.

References

1 World Health Organization (2022). *Global Tuberculosis Report.* World Health Organization: Geneva, Switzerland. Licence: CC BY-NC-SA 3.0 IGO. https://www.who.int/teams/global-tuberculosis-programme/tb-reports/global-tuberculosis-report-2022

2 Scior, T., Morales, I.M., Eisele, S.J.G., Domeyer, D., & Laufer, S. (2022). Antitubercular Isoniazid and Drug Resistance of Mycobacterium tuberculosis — A Review. *Arch. Pharm.*, *335*, 511–525. https://doi.org/10.1002/ardp.200290005

3 Narmandakh, E., Tumenbayar, O., Borolzoi, T., Erkhembayar, B., Boldoo, T., Dambaa, N., & Chiang, C.Y. (2020). Genetic Mutations Associated with Isoniazid Resistance in Mycobacterium tuberculosis in Mongolia. *Antimicrobial Agents and Chemotherapy*, *64*(7), Article e00537-20. https://doi.org/10.1128/aac.00537-20

4 Arun, K.B., Madhavan, A., Abraham, B., Balaji, M., Sivakumar, K.C., Nisha, P., & Kumar, R.A. (2021). Acetylation of Isoniazid Is a Novel Mechanism of Isoniazid Resistance in Mycobacterium tuberculosis. *Antimicrobial Agents and Chemotherapy*, *65*(1), Article e00456-20. https://doi.org/10.1128/aac.00456-20

5   Rather, M.A., Amin, S., Maqbool, M., Bhat, Z.S., Gupta, P.N., & Ahmad, Z. (2016). Preparation and In Vitro Characterization of Albumin Nanoparticles Encapsulating an Anti-Tuberculosis Drug-Levofloxacin. *Adv. Sci. Eng. Med.*, *8*, 912–917. https://doi.org/10.1166/asem.2016.1922

6   Tazhbayev, Y., Galiyeva, A., Zhumagaliyeva, T., Burkeyev, M., & Karimova, B. (2021). Isoniazid-Loaded Albumin Nanoparticles: Taguchi Optimization Method. *Polymers*, *13*(21), Article 3808. https://doi.org/10.3390/polym13213808

7   Tazhbayev, Y., Mukashev, O., Burkeyev, M., & Lozinsky, V. I. (2020). Synthesis and Comparative Study of Nanoparticles Derived from Bovine and Human Serum Albumins. *Polymers*, *12*(6), Article 1301. https://doi.org/10.3390/polym12061301

8   Ge, Z.H., Ma, R., Xu, G.X., Chen, Z., Zhang, D.F., Wang, Q., Ma, W. (2018). Development and In Vitro Release of Isoniazid and Rifampicin-Loaded Bovine Serum Albumin Nanoparticles. *Medical Science Monitor*, *24*, 473–478. https://doi.org/10.12659/msm.905581

9   Somasundaram, S., Ram, A., & Sankaranarayanan, L. (2014). Isoniazid and Rifampicin as Therapeutic Regimen in the Current Era: A Review. *J. Tuberc. Res.*, *2*, 40–51. https://doi.org/10.4236/jtr.2014.21005

10   Galiyeva, A., Daribay, A., Zhumagaliyeva, T., Zhaparova, L., Sadyrbekov, D., & Tazhbayev, Y. (2023). Human Serum Albumin Nanoparticles: Synthesis, Optimization and Immobilization with Antituberculosis Drugs. *Polymers*, *15*(13), Article 2774. https://doi.org/10.3390/polym15132774

11   Tazhbayev, Y., Mukashev, O., Burkeev, M., & Kreuter, J. (2019). Hydroxyurea-Loaded Albumin Nanoparticles: Preparation, Characterization, and In Vitro Studies. *Pharmaceutics*, *11*(8), Article 410. https://doi.org/10.3390/pharmaceutics11080410

12   Lomis, N., Westfall, S., Farahdel, L., Malhotra, M., Shum-Tim, D., & Prakash, S. (2016). Human Serum Albumin Nanoparticles for Use in Cancer Drug Delivery: Process Optimization and In Vitro Characterization. *Nanomaterials*, *6*(6), Article 116. https://doi.org/10.3390/nano6060116

13   Chen, X.T., Lv, G.Y., Zhang, J., Tang, S.C., Yan, Y.G., Wu, Z.Y., & Wei, J. (2014). Preparation and properties of BSA-loaded microspheres based on multi-(amino acid) copolymer for protein delivery. *International Journal of Nanomedicine, 9*, 1957–1965. https://doi.org/10.2147/ijn.s57048

14   Galiyeva, A.R., Tazhbayev, Y.M., Zhumagaliyeva, T.S., Sadyrbekov, D.T., Shokenova, S.S., Kaikenov, D.A., & Karimova, B.N. (2022). Polylactide-co-glycolide nanoparticles immobilized with isoniazid: optimization using the experimental Taguchi method. *Bulletin of the University of Karaganda-Chemistry,* (105), 69–77. https://doi.org/10.31489/2022Ch1/69-77

15   Alves, R., Reis, T.V.D., da Silva, L.C.C., Storpírtis, S., Mercuri, L.P., & Matos, J.D. (2010). Thermal behavior and decomposition kinetics of rifampicin polymorphs under isothermal and non-isothermal conditions. *Brazilian Journal of Pharmaceutical Sciences*, *46*(2), 343–351. https://doi.org/10.1590/s1984-82502010000200022

16   Michnik, A., Michalik, K., Kluczewska, A., & Drzazga, Z. (2006). Comparative DSC study of human and bovine serum albumin. *Journal of Thermal Analysis and Calorimetry*, *84*(1), 113–117. https://doi.org/10.1007/s10973-005-7170-1

17   Gunasekaran, S., Sailatha, E., Seshadri, S., & Kumaresan, S. (2009). FTIR, FT Raman spectra and molecular structural confirmation of isoniazid. *Indian Journal of Pure & Applied Physics*, *47*(1), 12–18.

18   Sharma, A., Puri, V., Kumar, P., Singh, I., & Huanbutta, K. (2021). Development and Evaluation of Rifampicin Loaded Alginate-Gelatin Biocomposite Microfibers. *Polymers*, *13*(9), Article 1514. https://doi.org/10.3390/polym13091514

19   Ivashchenko, O., Tomila, T., Ulyanchich, N., Yarmola, T., & Uvarova, I. (2014). Fourier-Transform Infrared Spectroscopy of Antibiotic Loaded Ag-Free and Ag-Doped Hydroxyapatites. *Adv. Sci. Eng. Med.*, *6*, 193–202. https://doi.org/10.1166/asem.2014.1473

20   Mandhar, P. & Joshi, G. (2015). Development of Sustained Release Drug Delivery System: A Review. *Asian Pacific Journal of Health Sciences, 2*(1), 179–185. https://doi.org/10.21276/apjhs.2015.2.1.31

21   Loiko, O.P., Herk, A.M. van, Ali, S.I., Burkeev, M.Z., Tazhbayev, Y.M., & Zhaparova, L.Z. (2013). Controlled release of Capreomycin sulfate from pH responsive nanocapsules. *e-Polymers, 13*(1). https://doi.org/10.1515/epoly-2013-0118

22   Burkeev, M.Z., Zhaparova, L.Z., Tazhbaev, E.M., Zhumagalieva, T.S., Ali, S.I. & van Herk, A.M. (2013). In Vitro Studies of Capreomycin Sulfate Release from Polyethylcyanoacrylate Nanoparticles. *Pharmaceutical Chemistry Journal, 47*(3), 154–156. https://doi.org/10.1007/s11094-013-0916-3